International Symposium of Research Students on Materials Science and Engineering
December 20-22, 2004, Chennai, India
Department of Metallurgical and Materials Engineering, Indian Institute of Technology Madras

PARTICLE SIZE COMPARISON OF SOFT-CHEMICALLY PREPARED NICKEL AND COPPER ALUMINATE SPINELS

Debasis Dhak and Panchanan Pramanik
Department of Chemistry, Indian Institute of Technology Kharagpur-721302, India

ABSTRACT

Nanocrystalline MAl_2O_4 (M=Ni and Cu) spinel powders are synthesized by pyrolysis of complex compounds of aluminium and transition metal (Nickel and copper) with triethanolamine (TEA). The precursor materials are formed on complete dehydration of the soluble complexes of aluminium-TEA and transition metal-TEA (copper and nickel) maintaining the resulting pH of each of the solution 4-5. The precursors are heat treated at different temperatures to provide phase formations. Single-phase $NiAl_2O_4$ spinel powders are resulted after heat treatment of the precursor material at 600^oC but for $CuAl_2O_4$, the precursor passes through an intermediate phase CuO at lower treatment temperature. The precursor and the heat-treated powders are characterized by XRD, FTIR, DTA-TG, TEM; surface area is measured by BET adsorption isotherm. The average particle sizes have been compared that are obtained from XRD, TEM and BET adsorption isotherm.

Keywords: Soft chemical, TEA, Spinels.

1. INTRODUCTION:

In recent years there has been increasing interest in the synthesis of nanocrystalline metal oxides [1-5]. In the search for improved properties of catalytic materials, great interest has been focused on spinel-type structures. Aluminates, among these materials seem to be a good option because of their properties such as high thermal stability, high mechanical resistance, hydrophobicity, and low surface acidity. These properties make them interesting materials as catalysts [6] and carriers for active metals to substitute the more traditional systems. Furthermore, it is known that some aluminate spinels, including zinc aluminate, copper aluminate tend to prevent sintering of noble metals due to a strong metal-support interaction [7]. The sintering resistance and chemical stability of catalytically active phases are a very important problem for high-temperature processes. Nickel and copper aluminate spinel (MAl_2O_4; M = Ni, Zn) may be used as a catalytic as well as a ceramic material. So far, it has been used as a catalyst for the decomposition of methane [8], for steam methane reforming reaction [9], dehydrogenation of n-hexanol [10], CO reduction by propane [11], preparation of polymethylbenzenes [12], methanol and higher alcohols synthesis [13-14], or the synthesis of styrenes from acetophenones [15], and foremost as a support for alkane dehydrogenation catalyst [15-18]. Zinc aluminate catalysts or supports and ceramics are commonly prepared by high temperature calcination (above 1000 K) of mixed aluminium and zinc oxides [19], coprecipitated products [20] sol-gel product [21-22], hydrothermal synthesis [23-27]or products of impregnating a porous alumina having a high surface area with a solution of zinc compound [28-29]. A disadvantage of such materials for catalytic applications is the low surface area, usually about 20–50 m2/g [30], where conventional catalyst or supports are porous materials whose surface area require comprised between 100 and 300 m^2/g. Better results may be obtained by sol-gel methods: MAl_2O_4 (M = Ni, Cu) spinels were prepared from single-source heterobimetallic alkoxides precursors by micro emulsion mediation.

Various mixed oxides with single phase and controlled particle size and morphology can be synthesized by organic precursor techniques. We describe here the synthesis and characterization of nano-spinels MAl_2O_4 (M^{II}= Ni, Cu). Aluminium based spinels constitute an interesting class of oxide ceramics with important technological applications. Although several chemical routes exist for the preparation of MAl_2O_4 powders, [31-33] the preparation of transition metal–aluminium spinels is limited to fusion of the two component oxides at high temperatures (1000–1600 °C) [34-36] or by co-precipitation reactions in solution. [37-38]. Moreover, no literature precedence, to our knowledge, is available on the synthesis and characterization of nano-scaled transition metal aluminates by a molecular precursor route. Presently, we report an organic precursor method or soft chemical method for the preparation of nanoporous transition metal aluminate spinels with a high surface area particularly useful for catalytic applications.

2. EXPERIMENTAL PROCEDURE

2.1. Synthesis of the spinel ceramics

The chemicals required are $Al(NO_3)_3$ $9H_20$ (E. Merck India Limited, 98%), $Ni(NO_3)_2$ $6H_2O$ (E. Merck India Limited, 99%), triethanolamine (TEA) (Qualigen Fine Chemicals, India), and HNO_3 (S. D. Fine Chemicals, India). Stoichiometric amounts of $Al(NO_3)_3$ $9H_2O$ and $Ni(NO_3)_2$ $6H_2O$ are mixed in such a way that the A1 to Ni ratio is maintained at 2:1. Aluminum nitrate and nickel nitrate solids are assayed by 8-hydroxyquinoline. After the concentrations of $A1^{3+}$ and Ni^{2+} in the solid are known, the solids are admixed in such a way that the aluminum to nickel ratio is maintained at 2:1. A small amount of water is added to it to form a pasty mass. Then the requisite amount of TEA is mixed to this pasty mass in such a way that the total metal ion ($A1^{3+}$ and Ni^{2+}) to TEA mole ratio is maintained at 1:3. At the beginning TEA forms precipitate (due to the formation of $A1^{3+}$ and Ni^{2+} hydroxides) with metal ions. This precipitate is dissolved and a clear solution is obtained by adding a certain amount of HNO_3 maintaining the pH at 3-4. The clear solution of TEA complexed metal nitrate is evaporated on a hot plate at 180^{o}C with constant stirring. Continuous heating of the solution causes foaming and puffing. During evaporation the nitrate ions provide an in situ oxidizing environment for TEA, which converts partially the hydroxyl groups of TEA to carboxylic acids. When complete dehydration occurs, the nitrates themselves are decomposed with the evolution of brown fumes of nitrogen dioxide, leaving behind a voluminous, organic-based, black, fluffy powder, i.e., precursor powder. The precursor powders after grinding are calcined at various temperatures to get a series of $NiA1_2O_4$ powders. $CuA1_2O_4$ is also prepared by the same procedure maintaining the same reaction conditions. The total preparation procedure is schematically shown in the figure 1. The heat treatments of the precursor materials (in air, 2 h) have been facilitated at various temperatures from 500^o C to 900^{o}C at a heating rate of 8-10 ^{o}C/min.

2.2. Powder characterization

Thermal gravimetric and differential thermal analysis (TG-DTA) (Model DT-40, Shimadzu Co., Kyoto, Japan) was performed from ambient temperature to 1000^{o}C at a heating rate of 10^{o}C/min using α-alumina as a standard in air atmosphere. The powders are characterized by X-ray diffraction (XRD) (Model PW 1710 and PW 1810, Philips Research Laboratories) using CuKα radiation. The crystallite size was calculated from line broadening of (311) diffraction line according Scherer equation. The lattice parameters were measured from the (311) diffraction line using Si as an internal standard. Infrared spectra were collected using a Perkin-Elmer 1600 FT-IR spectrometer. Spectra were obtained using KBr disks containing ~1% sample. Elemental composition was determined by Energy Dispersive X-ray (EDX) analysis (Model JFM 5800

JEOL Tokyo, Japan), in vacuum, in the specimen chamber of an EDX coupled scanning electron microscope. The TEM images were recorded on a transmission electron microscope (Model JEM-2010, JEOL, Tokyo, Japan) by drawing a carbon coated copper grid through the suspensions of various ceramics in acetone. The specific surface area was measured by the BET method in a BECKMAN COULTER analyzer. Before N_2 adsorption desorption measurement, each sample was degassed with a N_2 purge at 77 K for 3 hrs.

3. RESULTS AND DISCUSSION

3.1. TG-DTA Study

Thermogravimetric and differential thermal analysis (TG-DTA) curves of copper aluminate precursor powder is shown in figure 2.The total weight loss amounts to ~90% of the total precursor mass and occurs in a three step processes: (i) initial weight loss resulting from the evaporation of adsorbed water; (ii) a significant weight loss results from the pyrolysis of the organic compounds (TEA) which is observed as the prominent exothermic peak in the DTA curve at ~ 420^{o}C. From the graph it is also observed that the metal-TEA precursor powder exhibits weight loss up to 600 ^{o}C (iii) a third weight loss occurring gradually over a wide range of temperature attributed to pyrolytic elimination of amines, entrapped gases, as indicated by a broad line between 600 to 750 ^{o}C. Here the weight loss becomes almost constant. This indicates that below 590^{o}C, metal complexes along with unreacted amine decompose. The whole thermal process is associated with the evolution of a large amount of gases (such as CO, CO_2, NH_3, NO_2, NO and water vapor) that is reflected by the total weight loss of 90% in the TGA curve.

3.2. XRD Study

The effect of different treatment temperatures on the solid phase changes using $NiAl_2O_4$ and $CuAl_2O_4$ precursors are shown in figure 3 and 4 respectively. In order to restrict crystallite growth, the calcination times at a fixed heating rate were carefully monitored to keep them as short as possible. The diffratograms of all the samples calcined at 900^{o}C indicate that each sample is a monophasic spinel [PCPDFWIN VERSION 2.02© copyright 1999 by ICDD Powder Diffraction Data base, File Card Nos. (78-1601) and (78-1605) respectively for $NiAl_2O_4$, and $CuAl_2O_4$]. For both these two metal aluminates, substantial crystallinity is achieved at 900^{o}C after calcination of the amorphous raw product for 30 minutes. However crystallization is also possible at much lower temperatures. No peak sequence can be attributed either to nickel or aluminium oxides or carbonates, nitrates, or to known nickel-aluminium mixed compounds, could be found in the XRD pattern of the precursor. In contrast to $NiAl_2O_4$, the raw precursor powder for $CuAl_2O_4$ spinel exhibit a different thermal behavior, which is shown in figure 4. The amorphous raw product does not transform into a pure aluminate phase. Rather an intermediate CuO phase becomes evident at 700^o C, which diminishes with increasing temperature and non existent at 800^o C. This tendency of phase separation has been observed only during the processing of copper aluminate. At 800^{o}C, the CuO phase is no longer present and the diffraction pattern reveals monophasic $CuAl_2O_4$ (figure 4). Further details understanding for the formation and conversion of the CuO phase are currently in progress.

3.3. IR Study

The IR spectra of the MAl_2O_4 powders (M= Ni and Cu) in all four cases, show metal-oxygen stretching frequencies in the range 500-900 cm^{-1}associated with the vibrations of M-O, Al-O and M-O-Al bonds. [39-42]. No significant peak is present in the frequency region 1028-1157cm^{-1}, which confirms the absence of Al-OH bending mode. All raw products show broad and intense hydroxyl stretching frequencies [υ(OH)] which can be assigned to the overlapping

of bands due to surface adsorbed water (*ca*.3400 cm^{-1}). The small peaks at around 1384 cm^{-1} and 2857-2920 cm^{-1} correspond to the presence of trace amount of CH_2 and C-H band. The peak at 1624.74 cm^{-1} is probably due to the deformation of water molecules [$\partial(H_2O)$] of powders or due to the presence of acid CO which has not been decomposed completely during heating. The powders in every case obtained in low temperature shows the peak at 2361.8 cm^{-1} which is due to the asymmetric stretching frequency [υ(CO)] of CO_2 .The presence of this CO_2 is caused either due to the aerial CO_2 or may be due to the presence of CO_2 inside the grains of powders. Residual organic and hydroxyl groups evident in raw powders are absent in the calcined samples of $NiAl_2O_4$ while $CuAl_2O_4$ shows, even after calcination at 800°C, residual C–H and C-N bands as corroborated by the C H N analyses of the calcined samples (see below). The IR spectra of $CuAl_2O_4$ powders calcined at lower and at higher treatment temperature (500°C and 800°C) are shown on figures 6 and 7. The symmetric C–O stretching frequency at 1632cm^{-1} in the raw powders is due to the formation of acid during the oxidation of tri-ethanol amine (TEA) in presence of nitric acid. The intensity of υ(OH) bands decreases on firing the raw material and at 500°C the sample contains no hydroxyl groups. The appearance of a broad υ(OH) band is probably due to absorption of water during pelletization with KBr. On comparison with the IR spectral pattern reported [38] for $MgAl_2O_4$ and other substances with spinel-like structures, the two Al–O stretching bands observed in the range 500–900 cm^{-1} can be assigned to different coordination states of Al atoms (AlO_6 and AlO_4 units). It is probable that the transition metal–oxygen vibrations of the spinels overlap with the Al–O bands. The IR spectra of the raw powders and heat-treated samples of $CuAl_2O_4$ s are broader compared to $NiAl_2O_4$.

4. POWDER CHARACTERISTICS AND THE PARTICLE SIZE COMPARISON

The energy dispersive X-ray (EDX) analysis of the powders calcined at their phase formation temperatures performed on several spots shows that there is no detectable variation in the elemental composition at the submicrometer level. The elemental compositions determined for all four systems are within 2% of the intended stoichiometry. Nickel aluminate after calcination at 600°C (2hr) is found to be free from organic contaminations (carbon, nitrogen, and hydrogen contents less than 0.3%) while the copper aluminate sample shows a significant amount of carbon (C, 5.2%: H, 3.9%).

The XRDs of the powders have already been described earlier; the FWHM for (311) reflection plane (full width half maximum) at different temperatures for nickel aluminate is plotted in figure 8, which shows the decreasing trend of FWHM very slowly through the entire treatment temperature range. This indicates that the crystallinity of $NiAl_2O_4$ is improved with increasing treatment temperatures in the temperature range studied in figure 9.
The cell constants of the powders obtained after treating the precursors at different temperatures have been calculated and compared with their theoretical values shown by the table I. Both nickel and copper aluminate crystal lattices are found to be expanded by 0.64686% and 0.5768%, respectively for $NiAl_2O_4$ and $CuAl_2O_4$.

Transmission electron photographs of the heat-treated powders are shown. The photographs of nickel and copper aluminates in figure10 and figure12 respectively show that the particles are uniform and non-aggregated with fairly narrow distributions. Whereas figures 11 and 13 show the agglomerates of nickel and copper aluminates respectively.

The average particle size of 5.10 nm, calculated from BET, is smaller than that calculated by XRD method (5.64 nm) for 600°C treated $NiAl_2O_4$ sample. For both the cases as shown by the table II, the particle diameter from TEM is found to be higher values compared to the values obtained from XRD and BET, which are probably due to the formation of agglomerates during dispersion in acetone at the time of sample preparation.

5. PLAUSIBLE MECHANISM OF THIS SYNTHETIC PROCEDURE

The preparation procedure involves the evaporation of aqueous precursor solutions that are composed of stoichiometric amounts of the desired metal ions, complexed with TEA. TEA is an efficient chelating agent that has good coordination properties with the metal-ions. 1-2 moles of TEA per mole of the total metal ions are stoichiometrically required for formation of stable complexes with metal ions. However, TEA in the precursor solution has always been kept in excess to the required stoichiometry. During evaporation of the precursor solution, the TEA present in the system probably led to the formation of vinyl functional groups that cause polymerization. The role of free TEA towards generation of the highly branched polymeric structure can be represented by the following tentative chemical reaction:

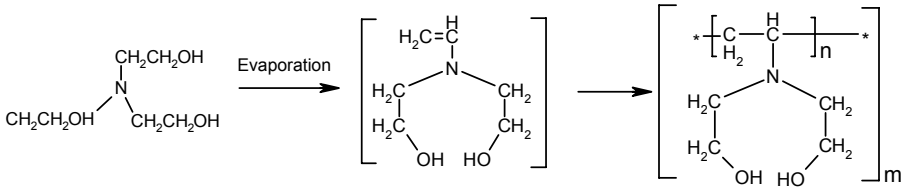

The water-soluble, metal ions/ metal coordinated complexes get uniformly anchored in the generated polymeric network structure and this possibly served to avoid their segregation or, any intermittent precipitation from the homogeneous precursor solution during evaporation.

Complete evaporation of the precursor solution resulted in a highly branched polymeric structure with the metal ions homogeneously lodged in its matrix, which probably served as a template for the generation of a voluminous matrix of polar mesoporous-carbon rich precursor mass on oxidation. This nitrogen atom enriched precursor mass of mesoporous carbon favored the accommodation of the metal ions/ metal ion-complexes in its matrix.

Slow volatilization of this mesoporous carbonaceous residue in the precursors, through low temperature calcination in dynamic air oxidation (at temperature varying from 500 to 900^{o}C) provided the condition for the synthesis of the nano-particles of the respective mixed-oxide systems. The removal of residual carbon is also facilitated by the catalytic activity generated by the presence of transition metal ions with variable oxidation states.
The formation of mesoporous carbon and desired oxide forms can probably be visualized through the following tentative chemical reaction:

Next, the reaction between the coordinated metal complexes with the polymeric structure generated from polymerization of free TEA can be represented by

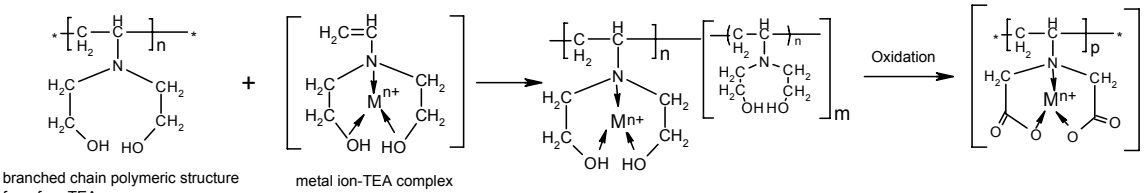

where 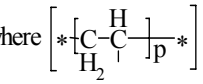 is the polymerized unit and M = metal ion

Next,

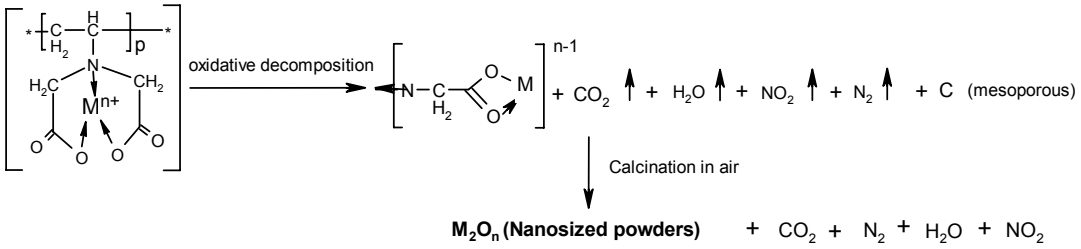

Thus, the chelating / complexing agents used play a dual role. They not only serve to keep the metal ions uniformly distributed throughout the viscous liquid during evaporation but also help to form the fluffy, voluminous, mesoporous carbon rich precursor material. The mesoporous carbonaceous precursors provide heat by combustion during pyrolysis and facilitated the reduction of the external temperatures required for the desired phase formation. The entire oxidative decomposition process is accompanied by the evolution of large amounts of gases (such as: water vapor, CO, CO_2, etc.), which help the precursor material to dissipate the heat of combustion and thus inhibit the sintering of the fine particles during the process.

6. CONCLUSION

The following conclusions can be drawn from the experiments cited in this paper.

- All the ceramics obtained are monophasic and exhibit well developed spinel phases after remarkably short calcination time periods.
- The particles size obtained by this soft chemical method can be monitored by varying the amount of TEA used, P^H of the resulting solution, heat treat temperature and duration of heating.
- These types of catalyst with high surface areas having narrow distributions of particle are possible to prepare by this soft chemical method which is cost effective and easy to prepare.
- The compound prepared with such an excellent surface area can be used for promising catalytic activity.

7. ACKNOWLEDGEMENT:

The authors are grateful to the Council for Scientific and Industrial Research (CSIR), New Delhi, India for the financial grant offered in support of this work

REFERENCES

1. R. N. Das, A. Pathak, and P. Pramanik, J. Am. Ceram. Soc., 81 [12] 3357-60 (1998).
2. K. Suresh and K. C. Patil, J. Solid State Chem., 99, 12-17 (1992).
3. Adak, A. Pathak, and P. Pramanik, J. Mater. Sci. Lett., 17 [7] 559-61 (1998).
4. P. Pramanik, Bull. Mater. Sci., 18 [6] 819-29 (1995).
5. P. Pramanik, Bull. Mater. Sci., 19 [6] 957-61 (1996).

6. J. Wrzyszcz, M. Zawadzki, J. Trawczynski, H. Grabowska and W. Mista. Applied Catalysis, A: General (2001), 210(1, 2), 263-269.
7. G. Aguilar-Ros, M.A. Valenzuela, H. Armendariz, P. Salas, J.M. Dominguez, D.R. Acosta, I. Schifter, Appl Catal A: General 90 (1992) 25–34.
8. Lingyu Piao, Yongdan Li, Jiuling Chen, Liu Chang and Jerry Y. S. Lin. Catalysis Today (2002), 74(1-2), 145-155.
9. T. Numaguchi, H. Eida and K. ShojiInternational Journal of Hydrogen Energy (1997), 22(12), 1111-1115.
10. Grabowska, H.; Zawadzki, M.; Wrzyszcz, J. Polish Journal of Chemistry (2003), 77(6), 779-787.
11. Danchevskaya, M. N.; Torbin, S. N.; Murav'eva, G. P.; Bol'shakov, A. M. Kafedra Fiz. Khim. Seriya 2: Khimiya (2002), 43(5), 288-290.
12. L.R. Cobb, Preparation of polymethylbenzenes, U.S. Patent 4,568,784, 1985
13. F. Le Peltier, P. Chaumette, J. Saussey, M.M. Bettahar, J.C. Lavalley, Mol Catal A: Chemical 122 (1997)131–139.
14. R. Szymanski, Ch. Travers, P. Chaumette, Ph. Courty, D. Durand, in: B. Delmon, P. Grange, P.A. Jacobs, G. Poncelet (Eds.), Studies in Surface Science and Catalysis, Vol. 31, Elsevier, Amsterdam, 1987, pp.739–748
15. R. Roesky, J. Weiguny, H. Bestgen, U. Dingerdissen, Appl Catal A: General 176 (1999) 213–220
16. M.A. Valenzuela, P. Bosch, G. Aguilar-Rios, B. Zapata, C. Maldonado, I. Schifter, J Mol Catal 84 (1993) 177–186.
17. G. Khare, R.A. Porter, U.S. Patent 5,430,220, 1995.
18. P.F. Schubert, D.H. Kubicek, D.R. Kidd, U.S. Patent 5,151,401,1992
19. W.-S. Hong, L.C. De Jonghe, J Am Ceram Soc 78 (12) (1995) 3217–3224.
20. G. Aguilar-Rios, M. Valenzuela, P. Salas, H. Armendariz, P. Bosch, G.Del Toro, R. Silva, V. Bertin, S. Castillo, A. Ramirez-Solis, I. Schifter, Appl Catal A.: General 127 (1995) 65–75.
21. Daniele, S.; Tcheboukov, D.; Pfalzgraf, L. G. Hubert. Journal de Physique IV: Proceedings (2001), 11(Pr11, TFDOM 2, International Conference on Thin Film Deposition of Oxide Multilayers Hybrid Structures, 2001), 283-287.
22. Sanjay Mathur, Michael Veith, Michel Haas, Hao Shen, Nicolas Lecerf, Volker Huch, Stefan Hüfner, Robert Haberkorn, Horst P. Beck, and Mohammad Jilavi. Journal of the American Ceramic Society (2001), 84(9), 1921-1928.
23. Zhizhan Chen, Erwei Shi, Wenjun Li, Yanqing Zheng, Nanchun Wu, and Weizhuo Zhong. Journal of the American Ceramic Society (2002), 85(12), 2949-2955.
24. Research on Chemical Intermediates (2003), 29(2), 137-146.
25. Zhi-Zhan Chen, Er-Wei Shi, Yan-Qing Zheng, Bing Xiao, and Ji-Yong Zhuang. Journal of the American Ceramic Society (2003), 86(6), 1058-1060.
26. M. Zawadzki and J. Wrzyszcz. Materials Research Bulletin (2000), 35(1), 109-114.
27. Zhizhan Chen, Erwei Shi, Yanqing Zheng, Wenjun Li, Nanchun Wu and Weizhuo Zhong Materials Letters (2002), 56(4), 601-605.
28. D.W. Walker, Zinc aluminate prepared using an alumina hydrate, U.S. Patent 4,370,310, 1983.
29. G.B. Carrier, Process for producing porous spinel materials, U.S. Patent 4,256,722, 1981.
30. M.A. Valenzuela, J.P. Jacobs, P. Bosch, S. Reijne, B. Zapata, H.H. Brongersma, Appl Catal A: General 148 (1997) 315–324
31. A. K. Adak, S. K. Saha and P. Pramanik, *J. Mater. Sci. Lett*., 1997, 16, 234.
32. M. Barj, J. F. Bocquet, K. Chhor and C. Pommier, *J. Mater. Sci*., 1992, 27, 2187.
33. R. E. Rocheleau, Z. Zhang, J. W. Gilje and J. A. Meese- MarktscheVel, *Chem.Mater*., 1994, 6, 1615.
34. J. W. Mellor, *Trans. Ceram. Soc*., 1937, 36, 1.

35. J. A. Hedvall and J. Heuberger, *Z. Anorg. Allg. Chem*., 1921, 116, 137.
36. R. Rieke and W. Paetsch, *Ber. Dtsch. Keram. Ges.*, 1922, 3, 14
37. J. E. Baker, R. Burch and N. Yugin, *Appl. Catal.*, 1991, 73, 135.
38. T. Ohgushi and S. Umeno, *Bull. Chem. Soc. Jpn*., 1987, 60, 4457
39. G. A. Sigel, R. A. Bartlett, D. Decker, M. M. Olmstead and P.P. Power, *Inorg. Chem.*, 1987, 26, 1773.
40. R. W. Adams, R. L. Martin and G. Winter, *Aust. J. Chem*., 1970, 20, 773.
41. A. K. Kruger and G. Winter, *Aust. J. Chem.*, 1970, 23, 1.
42. C. G. Barraclough, D. C. Bradley, J. Lewis and I. M. Thomas, *J. Chem. Soc.*, 1961, 2601.

TABLES

Table: I. Comparison of cell constants with their theoretical values (Cu Kα as standard)

Composition	Calcination temperature (^oC)	Cell constant (a)^o A (Experimental)	Cell constant (a)^{o}A (theoretical)	%lattice deviation from theoretical value
$NiAl_2O_4$	600,700, 800, 900	8.0285	7.9769	+0.64686
$CuAl_2O_4$	800	8.1256	8.079	+0.57680

Table II. Particle size of synthesized MAl_2O_4 (M = Co, Ni, Cu, Zn) powders

Composition	Phase formation temperature (^oC)	Specific surface area (m^2/g)	Average particle size (nm) from XRD[§]	BET[†]	TEM[‡]
$NiAl_2O_4$	600	250			
$CuAl_2O_4$	800	67			

[§]The crystallite size from XRD is calculated from X-ray line broadening of (311) diffraction line using Scherer equation (size= 0.9 λ/βcosθ, λ = wave length of the target used, θ = half of incident angle of scanning)
[†]The particle size from the BET method is calculated from d = 6/ρSw, where Sw is the BET specific surface area, d is the diameter of particles with spherical shape, and ρ is the density of the sample. The densities of the powders are shown in table II.
[‡]The particle size from TEM photograph is the average value from the observation of 50 particles for each case.

Table III. Density of MAl_2O_4 (M = Ni, Cu) powders

Composition	Heat treatment temperature (^oC)	Density (ρ gm/cc)
$NiAl_2O_4$	600	4.7
$CuAl_2O_4$	700	4.37

FIGURES

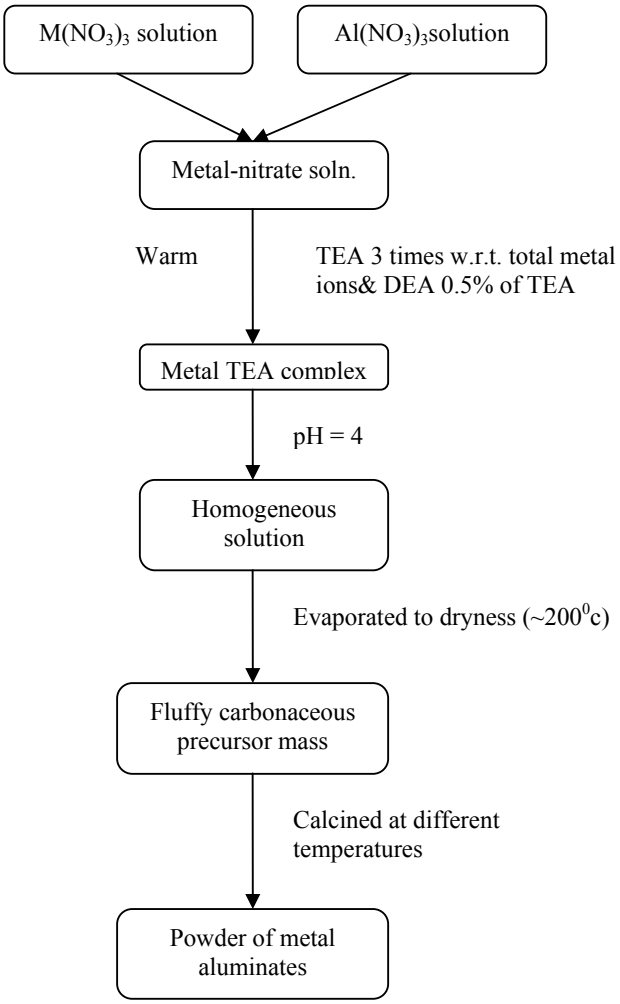

Figure 1 Schematic representation of preparation of MAl_2O_4 spinels (M= Ni, Cu)

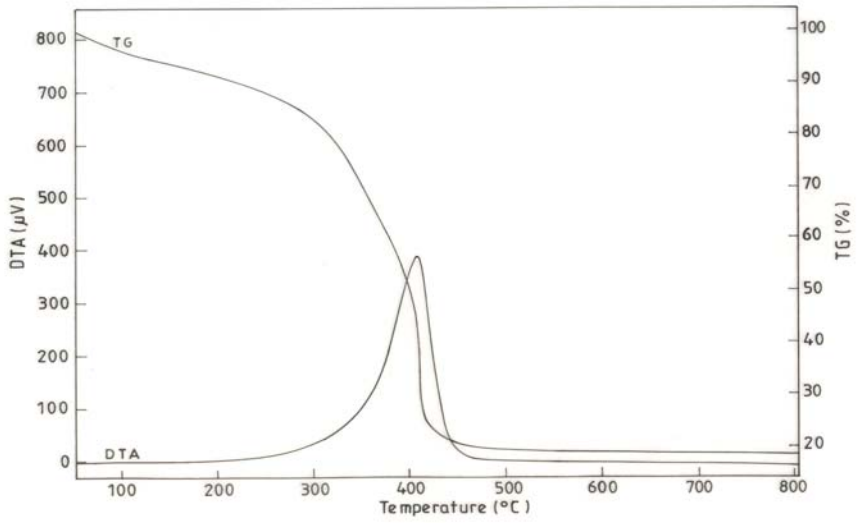

Figure 2 TG-DTA curve of $CuAl_2O_4$ precursor material

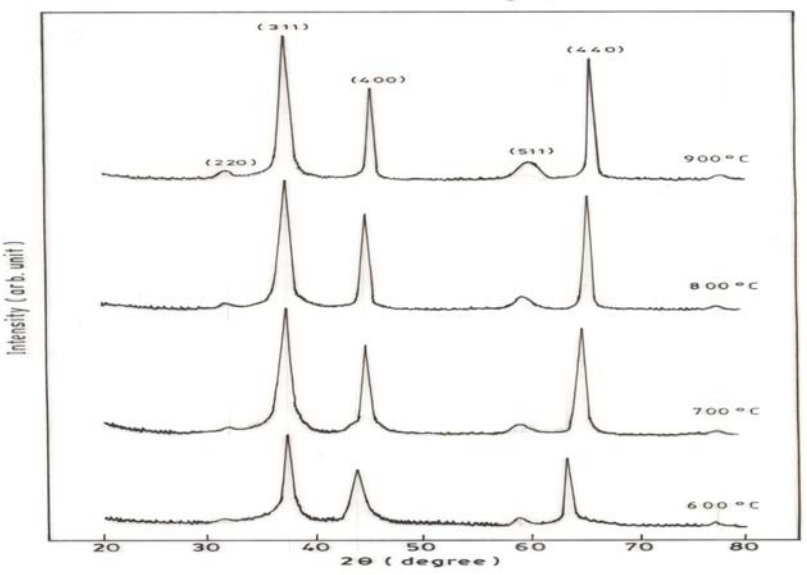

Figure 3 XRD patterns of $NiAl_2O_4$ powders obtained by heating the precursor in air for 2 h at 600°C, 700°C, and 800°C.

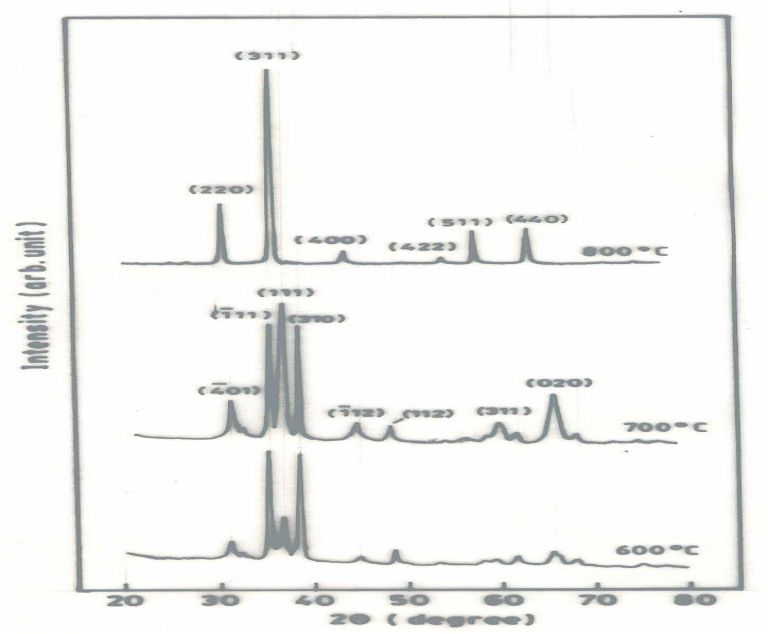

Figure 4 XRD patterns of $CuAl_2O_4$ powders obtained by heating the precursor in air for 2 h at 400°C 600°C, 700°C, and 800°C.

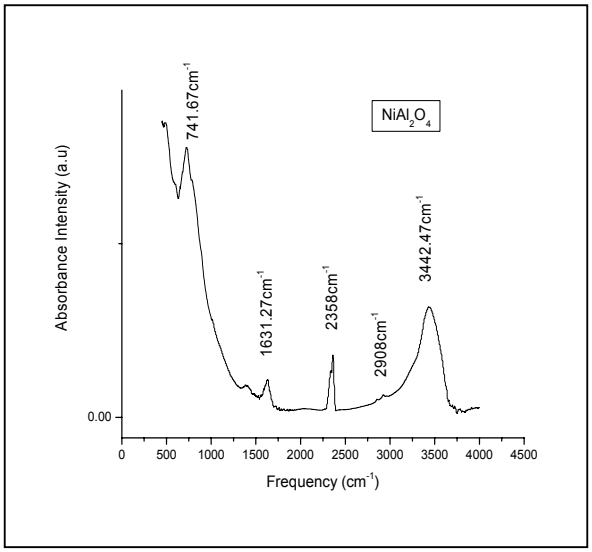

Figure 5 IR spectra of $NiAl_2O_4$ nano powder processed at 600°C temperature

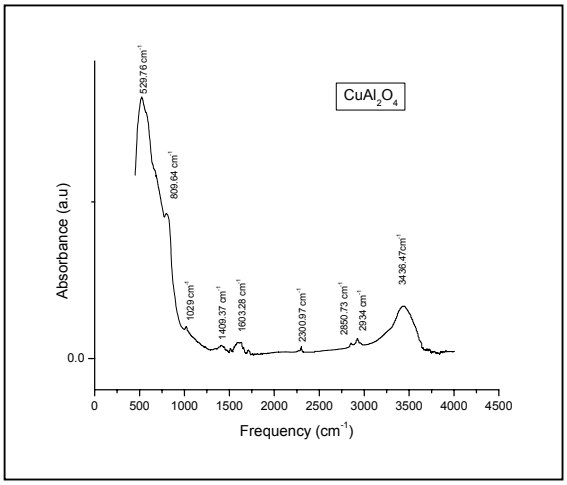

Figure 6 IR spectra of $CuAl_2O_4$ nano powder processed at 600^oC temperature

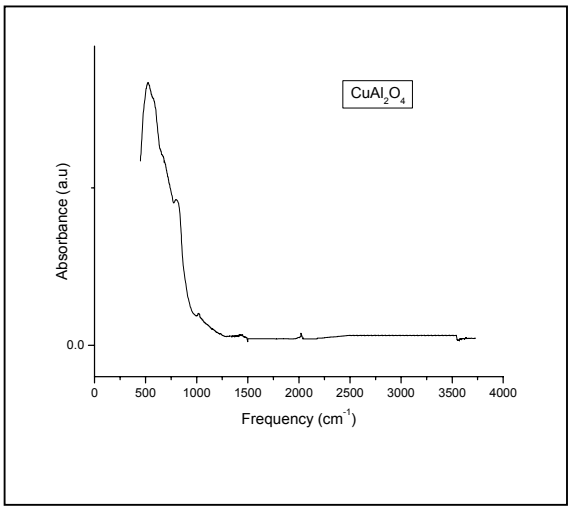

Figure 7 IR spectra of $CuAl_2O_4$ nano powder processed at 800^oC temperature

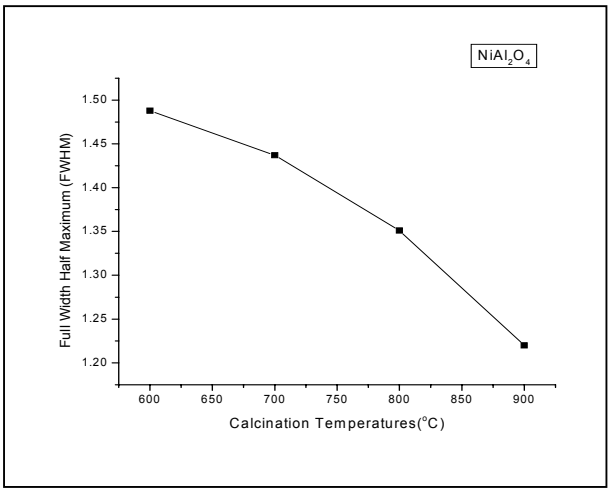

Figure 8 Plot of FWHM vs calcination temperature (^{o}C) of $NiAl_2O_4$ obtained from the peak position 2θ is equal to 55.54 degrees

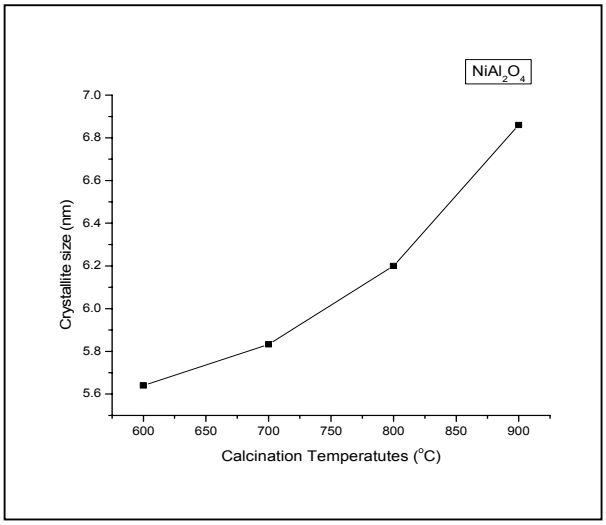

Figure 9 Plot of crystallite size obtained against the calcination temperatures (^{o}C) of $NiAl_2O_4$

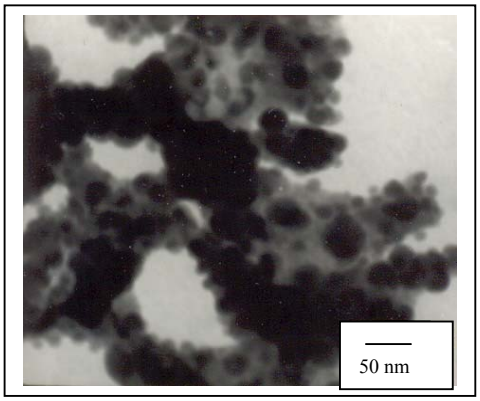

Figure 10 Bright field TEM image of $NiAl_2O_4$ powder calcined at 600^oC temperature showing the agglomerated particles.

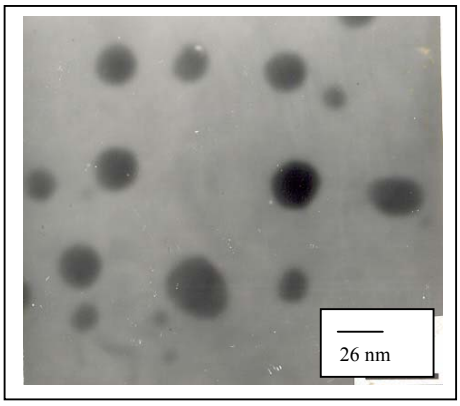

Figure 11 Bright field TEM image of $NiAl_2O_4$ powder calcined at 600^oC temperature showing few particles separately**.**

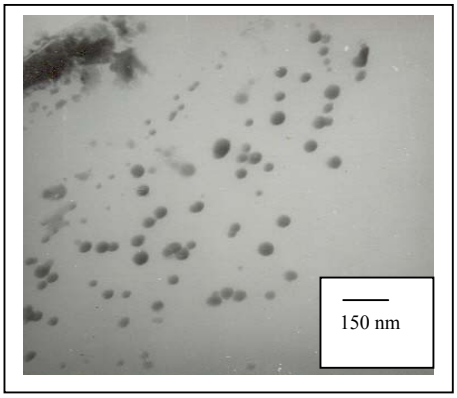

Figure 12 Bright field TEM image of $CuAl_2O_4$ powder calcined at 800^oC temperature showing both the agglomerated and some separated particles.

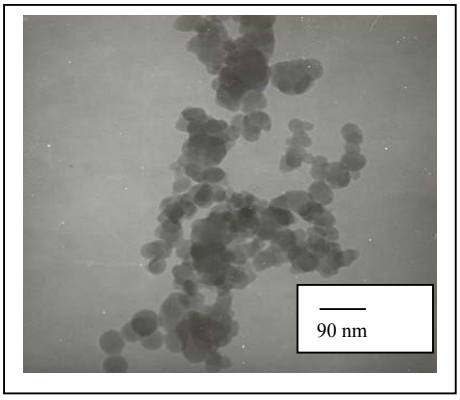

Figure 13 Bright field TEM image of $CuAl_2O_4$ powder calcined at 800^oC temperature showing few particles separately**.**